



RESEARCH ARTICLE

WILEY

In vitro characterization of iridoid and phenylethanoid glycosides from *Cistanche phelypaea* for nutraceutical and pharmacological applications

Antonella Delicato¹  | Marco Masi² | Francisco de Lara³ | Diego Rubiales⁴ |
 Ida Paolillo¹ | Valeria Lucci¹ | Geppino Falco¹ | Viola Calabrò¹  |
 Antonio Evidente²

¹Dipartimento di Biologia, Università di Napoli Federico II, Complesso Universitario Monte Sant'Angelo, Naples, Italy

²Dipartimento di Scienze Chimiche, Università di Napoli Federico II, Complesso Universitario Monte Sant'Angelo, Naples, Italy

³Farmstate Finca Torrecillas eco retreat, Murcia, Spain

⁴Institute for Sustainable Agriculture, CSIC, Córdoba, Spain

Correspondence

Viola Calabrò, Dipartimento di Biologia, Università di Napoli Federico II, Complesso Universitario Monte Sant'Angelo, Via Cintia 4, 80126 Naples, Italy.
 Email: vcalabro@unina.it

Abstract

“Desert hyacinths” are a remarkable group of parasitic plants belonging to genus *Cistanche*, including more than 20 accepted species typically occurring in deserts or coastal dunes parasitizing roots of shrubs. Several *Cistanche* species have long been a source of traditional herbal medicine or food, being *C. deserticola* and *C. tubulosa* the most used in China. This manuscript reports the isolation and identification of some phenylethanoid and iridoid glycosides, obtained from the hydroalcoholic extract of *C. phelypaea* collected in Spain. The present study aims to characterize the antioxidant activity of *C. phelypaea* metabolites in the light of their application in nutraceutical and cosmeceutical industries and the effect of acetoside, the most abundant metabolite in *C. phelypaea* extract, on human keratinocyte and pluripotent stem cell proliferation and differentiation. Our study demonstrated that acetoside, besides its strong antioxidant potential, can preserve the proliferative potential of human basal keratinocytes and the stemness of mesenchymal progenitors necessary for tissue morphogenesis and renewal. Therefore, acetoside can be of practical relevance for the clinical application of human stem cell cultures in tissue engineering and regenerative medicine.

KEYWORDS

antioxidants, *Cistanche*, *Cistanche phelypaea*, iridoid glycosides, phenylethanoid glycosides, nutraceuticals

1 | INTRODUCTION

The genus *Cistanche* includes more than 20 species that are holoparasites, lacking chlorophyll and functional leaves. They parasitize the

roots of halophytic perennial shrubs typically on deserts, arid lands, or coastal dunes (Xu et al., 2009). They are commonly known as “Desert hyacinths”. Besides their evolutionary or botanist interest, *Cistanche* species raised herbalist interest, having used in traditional Chinese medicine or food for more than 2000 years. However, its use in traditional medicine is not restricted to China, as it has also been used in

Antonella Delicato and Marco Masi equally contributed to this work.

This is an open access article under the terms of the [Creative Commons Attribution-NonCommercial-NoDerivs](https://creativecommons.org/licenses/by-nc-nd/4.0/) License, which permits use and distribution in any medium, provided the original work is properly cited, the use is non-commercial and no modifications or adaptations are made.

© 2022 The Authors. *Phytotherapy Research* published by John Wiley & Sons Ltd.

North African Sahara (Bougandoura et al., 2016; Lakhdari et al., 2016; Volpato, Saleh, & Di Nardo, 2015). The used product is known as “Herba cistanche” and is traded as dried stems of a mix of *Cistanche* species that are either wild-harvested or cultivated by growing the host shrubs (Thorogood et al., 2021). *C. deserticola* and *C. tubulosa* are “cultivated” in China with a harvest of about 6000 tons (Song, Zeng, Jiang, & Tu, 2021). There is prospect for extending *Cistanche* cultivation, as in addition to the demand of Herba cistanche, there is a demand for plantation of drought-tolerant shrubs to serve as stabilizing “shelter forests” as a possible solution to the global desertification. Suitable shrubs for this purpose, such as saxaul and tamarisk happen to be ideal hosts of *Cistanche*, offering opportunities to expand *Cistanche* co-cultivation (Salehi, Esmailzadeh, Kheyli, Malekshah, & Zaroudi, 2019) and relieving pressure on wild populations due to unsustainable harvesting. Predictions have been made on the potential adaptation of several *Cistanche* species to new target regions based on climate (Wang, Zhang, Du, Pei, & Huang, 2019). In this line, prospects for the cultivation of *C. phelypaea* are currently being explored in dry areas of South-Eastern Spain.

Composition and nutraceutical and pharmacological applications of *C. deserticola* and *C. tubulosa* are rather well studied, as they are widely used in China (Wang, Zhang, Du, Pei, & Huang, 2019), but this is less the case for *C. phelypaea*, a food resource for Saharan populations, having a more Mediterranean distribution (Gast, 2000). Acetoside was reported to be the main bioactive constituent in genus *Cistanche*; it possesses excellent biological activities including antioxidant (Li et al., 2018), anti-inflammatory (Qiao, Tang, Wu, Tang, & Liu, 2019), neuro-protective (Gu, Yang, & Huang, 2016), and anti-osteoporotic activity (Yang et al., 2019).

The first chemical investigation on *C. phelypaea* was carried out in 1993. Acetoside, 2'-acetylacetoside, pheliposide, and tubulicide were isolated from its ethyl acetate extract as the main components (Melek, El-Shabrawy, El-Gindy, & Miyase, 1993). Subsequently, a new iridoid, named phelypaeside, was isolated from the dried aerial parts of the same plant grown in Qatar (Deyama, Yahikozawa, Al-Easa, & Rizk, 1995). Additional chemical investigations on *C. phelypaea* compounds and other species above mentioned were performed (Trampetti et al., 2019). Recently, in *C. phelypaea* water extract, antioxidant activity, in vitro inhibitory activity against acetyl- (AChE) and butyrylcholinesterase (BuChE) for Alzheimer's disease treatment, α -glucosidase, α -amylase for diabetes, and tyrosinase for skin hyperpigmentation disorders were reported (Trampetti et al., 2019).

The traditional uses of *Cistanche* species now cover a wide range of applications such as healthy food additives in Japan and Southeast Asia (Morikawa et al., 2019), for the treatment of kidney deficiency and erectile dysfunction (Li, Jiang, & Liu, 2017) or female infertility and constipation in elderly people (Zhang, Wang, Zhang, Chen, & Liang, 2005).

Here, we report the isolation and identification of some phenylethanoid and iridoid glycosides, obtained from the hydroalcoholic extract of *C. phelypaea* collected in Spain. The present study aims to expand the knowledge on acetoside, the most abundant phenylethanoid glycoside in *C. phelypaea* extract, focusing on human

keratinocyte and pluripotent stem cells in the light of its application in cosmeceutical, nutraceutical, and pharmaceutical industries. Our study demonstrated that acetoside besides its strong antioxidant potential can preserve the stemness of human keratinocyte and mesenchymal progenitors necessary for tissue morphogenesis and renewal.

2 | MATERIALS AND METHODS

2.1 | General experimental procedures

Optical rotations were measured on a Jasco (Tokyo, Japan) P-1010 digital polarimeter; ^1H and ^{13}C nuclear magnetic resonance (NMR) spectra were recorded at 400/500 and 100/125 MHz on Bruker (Karlsruhe, Germany) or Varian (Palo Alto, CA, USA) spectrometers, respectively. Electrospray ionization (ESI) mass spectra and liquid chromatography (LC/MS) analyses were performed using the LC/MS TOF system AGILENT 6230B, HPLC 1260 Infinity. The HPLC separations were performed with a Phenomenex LUNA (C18 5u 150 \times 4.6 mm). Analytical and preparative Thin-Layer Chromatography (TLC) was performed on silica gel plates (Kieselgel 60, F₂₅₄, 0.25 and 0.5 mm, respectively) or on reverse phase (Whatman, KC18, F₂₅₄, 0.20 mm) (Merck, Darmstadt, Germany) plates and the compounds were visualized by exposure to UV light and/or iodine vapors and/or by spraying first with 10% H₂SO₄ in MeOH, and then with 5% phosphomolybdic acid in EtOH, followed by heating at 110°C for 10 min. CC: silica gel (Merck, Kieselgel 60, 0.063–0.200 mm) and C₁₈-reverse-phase silica gel. D-glucose and D-xylose standards were supplied from Sigma-Aldrich (Milan, Italy). The purity of the isolated compounds was >98% as ascertained by ^1H NMR and HPLC analyses.

2.2 | Plant material

The *C. phelypaea* is common in the Iberian Peninsula (Pujadas-Salvá & López-Saéz, 2002), being particularly common in Murcia province (López-Espinosa, 2022). The specimens included in this study were collected at farmstate Finca Torrecillas, Corvera, Murcia, Spain in March 2020, identified by Dr J.A. López-Espinos (pers. comm.) and then sliced and dried in a shadow open room for 15 days. The plant voucher is deposited in the same farmstate.

2.3 | Extraction and purification of metabolites

400 g of dried *C. phelypaea* bulbs was milled with a blender and extracted with a Soxhlet apparatus using EtOH (1 \times 500 ml, 12 h) obtaining 9.3 g of organic extract as an oily residue. This residue was dissolved in distilled H₂O (200 ml) and extracted with EtOAc (3 \times 200 ml) obtaining 4.4 g of organic extract that was further fractionated by column chromatography on silica gel eluted with CHCl₃/isoPrOH (9:1, v/v) yielding 11 homogeneous fractions (F1-F11). The residue (695.7 mg) of F5 was further purified by CC on silica gel,

eluting with EtOAc/MeOH/H₂O (85:10:5, v/v/v), yielding nine homogeneous fractions (F5.1-F5.9). The residue of F5.3 (62.9 mg) was further purified by preparative TLC eluting with EtOAc/MeOH/H₂O (85:10:5, v/v/v) affording 2'-O-acetylacetoside (**2**, 20.9 mg) as an amorphous solid. The residue (172.1 mg) of F5.4 was purified by CC on reverse phase eluted with MeCN/H₂O (3.5:6.5, v/v) affording acetoside (**1**, 30.1 mg) and tubuloside B (**3**, 5.5 mg). The residue (18.3 mg) of F5.8 was further purified by TLC on reverse phase eluting with MeCN/ H₂O (3.5:6.5, v/v) yielding bartioside (**4**, 14.9 mg). The residue (336.5 mg) of F7 was purified by CC on reverse phase eluting with MeCN/ H₂O (3.5:6.5, v/v) affording five fractions (F7.1-F7.5) yielding 6-deoxycatalpol (**5**, 7.48 mg) and glucoside (**6**, 1.50 mg). The purification process has been repeated five times to accumulate the pure compounds for chemical and biological characterization.

Acetoside (1): amorphous solid, $[\alpha]_{\text{D}}^{25}$ -67.4 (c 1.0, MeOH) (ref. Aligiannis et al., 2003 $[\alpha]_{\text{D}}^{25}$ -69.6 (c 1.0, MeOH)); ¹H and ¹³C NMR data are in agreement with those previously reported by Kobayashi et al., 1987 and Kim, Kim, Jung, Ham, & Whang, 2009; ESI MS (+): *m/z* 647 [M + Na]⁺.

2'-O-Acetylacetoside (2) amorphous solid, $[\alpha]_{\text{D}}^{25}$ -63.4 (c 0.3, MeOH) (ref. Li, Ishibashi, Satake, Oshima, & Ohizumi, 2003 $[\alpha]_{\text{D}}^{25}$ -65.2 (c 0.1, MeOH)); ¹H and ¹³C NMR data are in agreement with those previously reported by Kobayashi et al., 1987; Han et al., 2012; ESI MS (+): *m/z* 667 [M + H]⁺.

Tubuloside (3) amorphous solid, $[\alpha]_{\text{D}}^{25}$ -37.4 (c 0.5, MeOH) (ref. Kobayashi et al., 1987 $[\alpha]_{\text{D}}^{25}$ -39.0 (c 1.0, MeOH)); ¹H and ¹³C NMR data are in agreement with those previously reported by Kobayashi et al., 1987; ESI MS (+): *m/z* 667 [M + H]⁺.

Bartioside (4) amorphous solid, $[\alpha]_{\text{D}}^{25}$ -86.4 (c 0.5, MeOH) (ref. Venditti, Serrilli, & Bianco, 2013 $[\alpha]_{\text{D}}^{25}$ -89.0 (c 0.3, MeOH)); ¹H and ¹³C NMR data are in agreement with those previously reported by Kobayashi et al., 1987; Venditti, Serrilli, & Bianco, 2013; ESI MS (+): *m/z* 353 [M + Na]⁺, 330 [M + H]⁺.

6-Deoxycatalpol (5) amorphous solid, $[\alpha]_{\text{D}}^{25}$ -50.0 (c 0.3, MeOH) (ref. Yoshizawa, Deyama, Takizawa, Usmanghani, & Ahmad, 1990 $[\alpha]_{\text{D}}^{25}$ -50.1 (c 0.7, MeOH)); ¹H and ¹³C NMR data are in agreement with those previously reported by Arslanian, Harris, & Stermitz, 1985; Kobayashi, Karasawa, Miyase, & Fukushima, 1985; ESI MS (+): *m/z* 347 [M + H]⁺.

Glucoside (6) amorphous solid, $[\alpha]_{\text{D}}^{25}$ -150.0 (c 0.1, MeOH) (ref. Sticher & Weisflog, 1975 $[\alpha]_{\text{D}}^{20}$ -178.5 (c 0.7, MeOH)); ¹H and ¹³C NMR data are in agreement with those previously reported by Sticher & Weisflog, 1975; Kobayashi, Karasawa, Miyase, & Fukushima, 1985; ESI MS (+): *m/z* 333 [M + H]⁺.

2.4 | Acid Hydrolysis of compounds 1–6

The acid hydrolysis of compounds 1–6 was conducted as previously described (Cimmino et al., 2016). Briefly, the glycosides (5.0 mg) were separately dissolved in 0.1 M HCl solution and stirred at 80°C for 3 h. The reaction mixture was concentrated under a vacuum obtaining amorphous solids as residues. The sugar and aglycones yield is 50%.

Pure sugars were identified by co-TLC eluting with *iso*PrOH/H₂O (8.2 v/v) with standards and recording their specific optical rotation.

2.5 | Cell culture and reagents

HaCaT, spontaneously immortalized keratinocytes from adult skin, were purchased from Service Cell Line (GmbH, Eppelheim, CLS, Germany) and cultured as described (Amoresano et al., 2010; Vivo et al., 2017). A431 (ATCC-CRL1555) human epidermoid carcinoma cells were from American Type Culture Collection (ATCC, Manassas, VA, USA). According to the p53 compendium database (<http://p53.fr>), HaCaT cells contain mutant p53 (H179Y/R282W), while A431 cells contain only one p53 mutated allele (R273H). All mentioned cell lines (10–14 passages) were cultured in Dulbecco's Modified Eagle's Medium (DMEM, Sigma Chemical Co, St. Louis, MO, USA) supplemented with 10% fetal bovine serum (FBS, Hyclone Laboratories, Inc. Logan, UT, USA) at 37°C in a humidified atmosphere of 5% CO₂.

hTERT-immortalized adipose-derived mesenchymal stem cells (hMSCs) were purchased from American Type Culture Collection (ATCC SCRC-4000; Virginia, USA). Cells (3–4 passages) were cultured in DMEM high glucose supplemented with 10% South American Fetal Bovine Serum (FBS), 2 mM glutamine, 100 units/ml Penicillin/Streptomycin (Gibco), and maintained in a humidified atmosphere of 5% CO₂ at 37°C. Media, sera, and antibiotics for cell culture were from Thermo Fisher Scientific (Waltham, MA, USA). All cell lines were routinely tested for mycoplasma contamination and were not infected.

2.6 | Differentiation protocol

For HaCaT differentiation, cells were seeded in an RMPI medium. The day after seeding, the medium was changed in RMPI without FBS, and cells were treated with Ca²⁺ at 2 mM until the cells reach confluence.

For osteogenic differentiation, the previously stored cells were plated at 8 × 10³ cells/cm² on 0.2 μg/cm² human collagen I coating (Corning) in a growth medium for 3 days at 37°C, 5% CO₂ in a humidified incubator, changing the medium after 2 days, before replacing the growth medium with osteogenic media (StemPro Osteogenesis Differentiation Kits_ThermoFisher Scientific) and maintaining for up to 18 days, with media changes every 2–3 days.

2.7 | Western blot analysis

Western blot was performed as previously reported (di Martino et al., 2016; Vivo et al., 2017). Briefly, 20 μg of whole-cell extracts were separated by sodium dodecyl sulfate-polyacrylamide gel electrophoresis (SDS-PAGE), subjected to western blot, and incubated overnight at 4°C with antibodies. Antibodies against p21WAF, Cytokeratin (VIK-10), Cytokeratin (K1207), and β-actin were from Cell

Signaling Technologies (Boston, MA, USA), and Δ Np63 α from Abcam (Cambridge, UK). Each experiment was run in triplicate. Signal intensities of western blot bands were quantified by Quantity One analysis software (Version Number 2, Biorad Laboratories, London, UK) and analyzed by GraphPad Prism 8.0.2 software (GraphPad, San Diego, CA).

2.8 | DCFDA assay

Antioxidant activity of 1–6 metabolites was measured using 2′–7′ dichlorofluorescein diacetate (DCFDA), a non-fluorescent compound permeable to the cell membrane, which can be oxidized by reactive oxygen species (ROS) giving a fluorescent compound as previously described (Xiao, Powolny, & Singh, 2008). In brief, 3×10^5 cells were treated with 50 or 100 μ M of purified metabolites as indicated. The medium was removed after 4 h and 1 mM (3%) H_2O_2 was added for 45 min, 1.5, and 2.0 h. Cells were washed with PBS and a fresh medium with DCFDA (30 mM) was added for 45 min, then DCFDA was removed by washing in PBS 1 \times and the cells were harvested. The measurement of ROS was obtained using the Sinergy H4 microplate reader Gen5 2.07 (ThermoFisher, Waltham MA, USA). The fluorescence emitted from the cells treated with DCFDA was compared to the untreated cells. Trolox was used as a positive control. Values shown in the plot are mean \pm SD of sixfold determinations. The mean and the standard deviation were calculated on biological triplicates using GraphPad Prism 8.0.2 software (GraphPad, San Diego, CA).

2.9 | Cell viability assay

Cell viability was evaluated by measuring the reduction of 3-(4,5-dimethylthiazol-2) 2,5-diphenyltetrazolium bromide (MTT) to formazan by the mitochondrial enzyme succinate dehydrogenase (Van Meerloo, Kaspers, & Cloos, 2011). Briefly, 10×10^3 cells were seeded on 96-well plates and exposed to different concentrations of total extract or metabolites for 48 and 72 h. MTT/PBS solution (0.5 mg/ml) was then added to the wells and incubated for 3 h at 37°C in a humidified atmosphere. The reaction was stopped by removal of the supernatant followed by dissolving the formazan product in acidic isopropanol and the optical density was measured with Sinergy H4 microplate reader Gen5 2.07 (ThermoFisher, Waltham MA, USA) using a 570 nm filter. Under these experimental conditions, no undissolved formazan crystals were observed. Cell viability was assessed by comparing the optical density of the treated samples compared to the controls.

2.10 | Trypan blue assay

1 part of 0.4% trypan blue and 1 part of cell suspension were mixed. The mixture was allowed to incubate for \sim 3 min at room temperature. The mixture was loaded into a Bürker chamber and the dead cells and

the total number of cells were counted to evaluate the percentage of viable cells (Warren, 2015).

2.11 | Cell proliferation analysis

A total of 6×10^4 HaCaT and A431 cells were seeded in a 12-well plate; cells were serum-starved for 24 h; after starvation, total extract or acetoside were added at different concentrations. Every 24 h cells were gently rinsed with 1 \times PBS, trypsinized, and counted. The count was confirmed by Scepter 2.0 analysis (Millipore, Burlington, MI, USA) as previously described (Fontana, 2018).

2.12 | RNA extraction, cDNA preparation, and qRT-PCR

Total RNA was extracted using TRIzol reagent (Invitrogen) and cDNA was synthesized using iScript cDNA Synthesis kit according to the manufacturer's instructions (Bio-Rad, Hercules, CA, USA). 1 μ g of total RNA was used for each cDNA synthesis. Primer 3 software (<http://primer3.ut.ee/>) was used to design the oligo primers setting the annealing temperature to 59–61°C for all primer pairs. Oligo sequences are reported in Table. For gene expression analyses, 25 ng of cDNA was used for each PCR reaction with each primer pair (forward/reverse primers mix: 0.2 μ M, in a final volume of 25 μ l). Real time-qPCR analysis was performed using the iTaq™ Universal SYBR® Green Supermix (Bio-Rad, Hercules, CA, USA) in a 7500 Real-Time PCR System (Applied Biosystems, Foster City, CA, USA) under the following conditions: 2 min at 50°C, 10 min at 95°C, followed by 40 cycles of 15 s at 95°C, and 1 min at 60°C. The GAPDH probe served as a control to normalize the data. The gene expression experiments were performed in triplicate on three independent experiments and a melting analysis was performed at the end of the PCR run. To calculate the relative expression level, we used the 2–DDCT method.

Gene name	Forward primer 5′–3′	Reverse primer 5′–3′
ENG	AGCCCCACAAGTCTTGCG	GCTAGTGGTATATGTCACCTCGC
COL1A1	CCCCTGGAAAGAATGGAGATG	TCCAAACCACTGAAACCTCTG
OCN	GGCGCTACCTGTATCAATGG	TCAGCCAACCTCGTCACAGTC
ALPL	ACGTACAACACCAATGCC	GGTCACAATGCCACAGATT
RUNX2	CTGTGGTTACTGTCATGGCG	AGGTAGCTACTTGGGGAGGA
GAPDH	GGTATCGTGAAGGACTCATGAC	ATGCCAGTGAGCTCCCGTTCAG

PCR primers.

2.13 | Statistical analysis

Statistical analyses were carried out using the GraphPad Prism version 8.1.2 (<https://www.graphpad.com/scientific-software/prism/>). Data were represented as the mean \pm standard deviation and analyzed for

statistical significance using ordinary one-way analysis of variance (ANOVA) and multiple comparisons. For all tests, $p < 0.05$ was considered to indicate a statistically significant difference.

3 | RESULTS

3.1 | In vitro cytotoxicity test of *C. phelypaea* EtOAc extract and isolation of metabolites

The whole EtOAc extract obtained from the *C. phelypaea* aerial parts was preliminarily tested for cytotoxicity on human HaCaT keratinocytes by the MTT viability test. The MTT viability test measures the mitochondrial succinate dehydrogenase activity and its ability to convert MTT into blue/purplish formazan salts. The EtOAc extract was tested at concentrations between 0.001 and 1 mg/ml for 48 and 72 h. At concentrations up to 0.01 mg/ml and 48 h of treatment, the extract positively impacted cell viability (Figure 1a, left panel). However, the proliferation rate of cells was not significantly affected by the treatments thus indicating that the observed increase in cell viability was likely due to an improvement of cellular metabolism (Figure 1b). At higher concentrations, the cytotoxic effect became predominant (Figure 1a).

The low in vitro cytotoxicity of *C. phelypaea* extract prompted us to proceed with the isolation of pure metabolites. The EtOAc extract of *C. phelypaea* was chromatographed as detailed in the Experimental Section to afford six homogeneous compounds. By comparing their spectroscopic data (essentially ^1H and ^{13}C NMR) with those reported in the literature (Kim, Kim, Jung, Ham, & Whang, 2009; Kobayashi et al., 1987) they were identified as the phenylethanoid glycosides acetoside, 2'-O-acetylacetoside (Han et al., 2012; Kobayashi et al., 1987), and tubuloside B (Kobayashi et al., 1987) (1–3, Figure 2) and the iridoid glycosides bartsioside (Kobayashi, Karasawa, Miyase, & Fukushima, 1985; Venditti, Serrilli, & Bianco, 2013), 6-deoxycatalpol

(Arslanian, Harris, & Stermitz, 1985; Kobayashi, Karasawa, Miyase, & Fukushima, 1985), and glucoside (Kobayashi, Karasawa, Miyase, & Fukushima, 1985; Sticher & Weisflog, 1975) (4–6, Figure 2). Their identification was confirmed by the ESIMS spectra and comparing their specific optical rotation data with those reported in the literature. Furthermore, the acid hydrolysis of compounds 1–3 afforded D-glucose and D-xylose while that of compounds 4–6 only D-glucose by co-TLC with standard sugars samples and recording the specific optical rotation. Compounds 1–3 belong to the phenylethanoid glycosides (PhGs) class of natural substances (Tian et al., 2021), while compounds 4–6 belong to the iridoid class (Wang et al., 2020) both known to possess significant bioactivities including antiviral, hepatoprotective, antibacterial, neuroprotective, antitumor, antiinflammatory, and antioxidant among others (Dewick, 2009; Tian et al., 2021; Wang et al., 2020). Their co-existence in *Cistanche* as well as in many other plants is well-known despite their different structures and biosynthetic pathways.

3.2 | Acetoside is the main antioxidant compound in *C. phelypaea*

We evaluated the in vitro antioxidant activities of glycosides and iridoids (1–5) isolated from *C. phelypaea* in human immortalized HaCaT keratinocytes using a 2' – 7' dichlorofluorescein diacetate (DCFDA) assay. HaCaT keratinocytes represent an immortalized cell type that proliferates indefinitely and being untransformed it is still able to differentiate in culture under appropriate stimuli.

Briefly, we compared Reactive Oxygen Species (ROS) induced by 1 mM H_2O_2 (1 mM, 3%) in cells pretreated for 4 h with 50 and 100 μM with the following metabolites: acetoside also known as verbascoside (1), 2'-O-acetylacetoside (2), tubuloside B (3), bartsioside (4), 6-deoxycatalpol (5) and glucoside (6). A permeable vitamin E analog, TROLOX, was used as a positive control. The negative control was

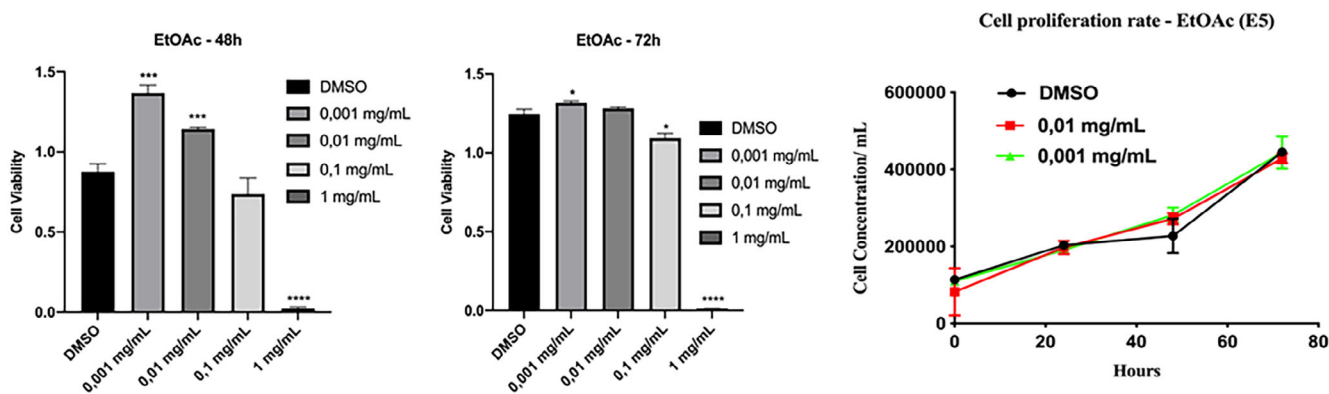


FIGURE 1 (a) MTT viability test. HaCaT cells were incubated with the indicated amount of EtOAc organic extract for 48 and 72 h. The values were the mean's six values for each experimental point of two independent biological replicates. Each mean was compared using a Dunnett's multiple comparisons test of ANOVA one-way (p -value < 0.01 , $** < 0.05$, $*** < 0.001$; $**** < 0.0001$). (b) Cell proliferation rate. HaCaT cells were plated and treated with EtOAc extract at the indicated concentrations. Following the treatment, they were counted with the Scepter cell counter, at times 0 and 24, 48, and 72 h, creating the proliferation curve. There is no significant change in the proliferation rate of the treated cells, compared to the DMSO control

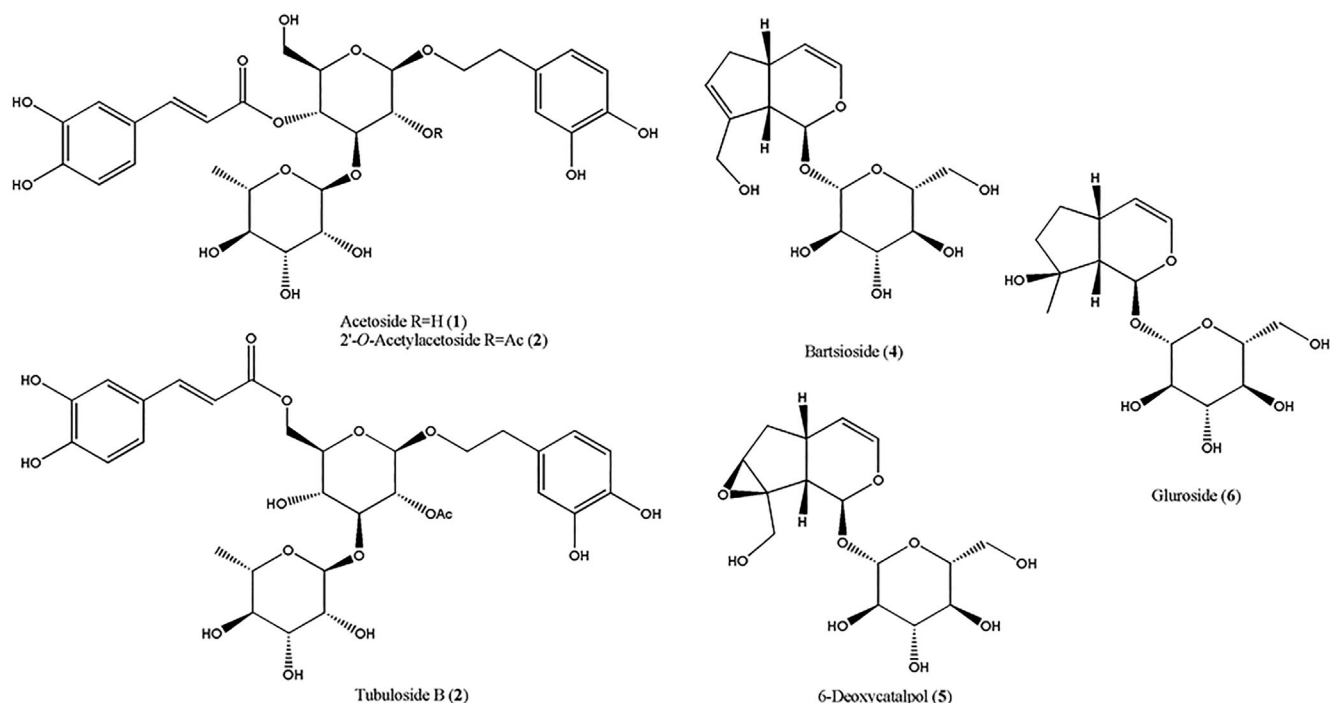


FIGURE 2 Structures of the phenylethanoid glycosides acetoside, 2'-O-acetylacetoside, and tubuloside B (1-3), and of the iridoid glycosides bartsioside, 6-deoxycatalpol, and glucoside (4-6), isolated from the EtOAc extract of *C. phelypaea*

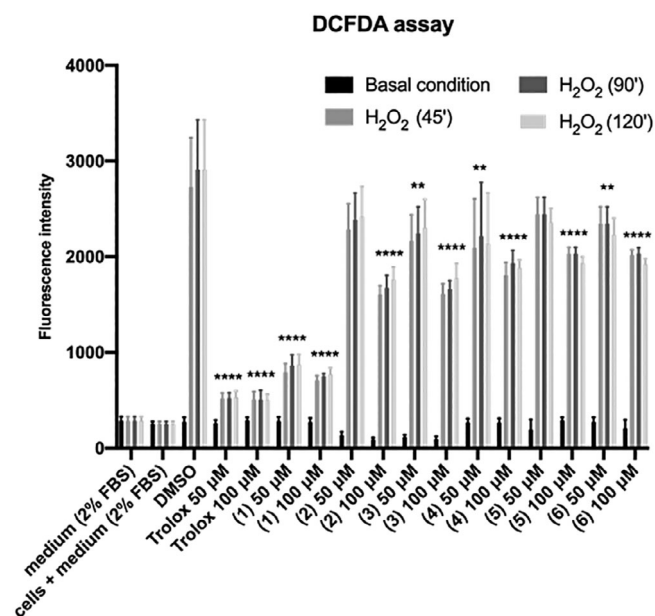


FIGURE 3 DCFDA assay. HaCaT cells were seeded and pre-treated for 4 h with 50 and 100 µM 1-6 metabolites from *C. phelypaea*. H₂O₂ (1 mM; 3%) was added to the medium for 45', 1.5, and 2 h. The fluorescence intensity of DCFDA was read after 45' of incubation. Trolox was used as a positive control and DMSO, in which the metabolites are dissolved, as a negative control. The values are the mean's six values for each experimental point of two independent biological replicates. Statistical analysis was performed with two-way ANOVA, using Tukey's multiple comparison test. Levels of significance between points of expression are indicated (*****p* < 0.001, ****p* < 0.01, ***p* < 0.05)

treated with the vehicle (DMSO 0.1%) used for diluting all compounds.

As shown in Figure 3, acetoside at a concentration of 50 and 100 µM dramatically reduced the level of ROS induced by H₂O₂ treatment. Pretreatment with 50 µM acetoside resulted in a 65% reduction of DCFDA fluorescence after 45' of treatment with H₂O₂. No further effects were observed by extending the treatment beyond 45' (Figure 3). This result was comparable to that obtained with an equal concentration of Trolox, the water-soluble derivative of vitamin E used as a positive control (Figure 3) thus indicating that acetoside has a strong radical scavenging activity. A reduction of intracellular ROS was also observed with all the other metabolites tested but it was moderate when compared to acetoside.

3.3 | Effect of *C. phelypaea* metabolites on cell proliferation and viability

The MTT assay is a widely used approach to measure the viability and proliferation of cells. However, the caffeoyl group of acetoside was shown to cause conflicting results in the MTT assay due to mitochondrial uncoupling effects (Wang, Zhou, Xu, & Gao, 2015). Therefore, we evaluated acetoside cytotoxicity on HaCaT keratinocytes and human A431 squamous carcinoma cells by the Trypan blue exclusion assay. The obtained results revealed that at the concentrations tested acetoside was not toxic for human keratinocytes while causing minimal cell death in tumor cells (between 12 and 20%) at the concentration of 100 µM (Table 1).

TABLE 1 Percentage of viable cells. HaCaT and A431 cells were seeded and treated with acetoside (1) 10, 50, 100 μ M. Dead cells were counted with Trypan Blue after 24, 48, 72 h from treatments, and the percentage of live cells was measured out of the total number of cells. Numbers are the average of triplicate data

A431 Time of incubation	% viability	100	50	10
24 h	96	95	93	90
48 h	94	80	97	97
72 h	96	88	95	98
Hacat Time of incubation	% viability	100	50	10
24 h	96	86	98	94
48 h	97	97	97	94
72 h	95	93	98	90

Moreover, we compared the cell proliferation rate of Hacat and A431 cells in acetoside containing medium and we consistently found a time and dose-dependent reduction in the rate of cell proliferation both in immortalized and transformed keratinocytes. Interestingly, carcinoma-derived cells were more sensitive than Hacat to the cell growth inhibitory effect of acetoside (Figure 4).

We also carried out the MTT assay on Hacat and A431 cells after treatment with increasing doses of iridoids glucosides 4, 5, and 6 from 10 to 100 μ M to evaluate their cytotoxicity. Data shown in Figure 5 indicate that Hacat keratinocytes are slightly sensitive to the toxicity effects of bartioside (4), 6-deoxycatalpol (5), and glucoside (6) while cell viability of A431 cancer cells was significantly reduced (less than 60%) after 48 of incubation with 100 μ M of 4, 5, and 6 (Figure 5, right panel). The observed reduction of cell viability was more pronounced at 48 of treatment thus revealing time-dependent toxicity of iridoids (Figure 5, compare left and right panel).

3.4 | Acetoside inhibits differentiation of human keratinocyte and pluripotent cells

The obtained results indicate that among the main compounds isolated from *C. phelypaea*, acetoside is the least toxic and the most effective against ROS production. Therefore, we explored the effect of acetoside on cell differentiation. Terminal differentiation of Hacat immortalized keratinocytes is coupled to cell cycle withdrawal, and this process has been associated with a transient up-regulation of the cell cycle inhibitor p21WAF. Upon Ca^{2+} stimulation, Hacat cells differentiate and express CK1 and CK10, the prominent suprabasal skin differentiation markers. To test the differentiation potential of HaCaT cells in presence of acetoside, we evaluated the expression of CK1 and CK10 as well as the expression of Δ Np63 α , a well-known epithelial stem cell marker. As shown in Figure 6, the addition of Ca^{2+} caused a reduction of Δ Np63 α and a concomitant increase of p21WAF, CK1, and CK10. In acetoside-treated keratinocytes, instead, we observed sustained p21WAF induction without an increase of CK1 and CK10 expression. Notably, the level of Δ Np63 α remained

unaffected (Figure 6). These observations suggest that acetoside can preserve keratinocyte stemness necessary for epithelial morphogenesis and renewal.

Data obtained on keratinocytes prompted us to investigate the activity of acetoside on pluripotent stem cells. Human mesenchymal stem cells (hMSC) can differentiate in osteoblasts using an in vitro differentiation protocol which is intended to recapitulate the osteogenic development in vivo. The hMSCs were induced to the osteogenic differentiation by replacing the basal medium with an osteogenic medium supplemented or not with acetoside at a concentration of 100 μ M for 16 days. Activation of the transcription of genes (such as COL1A1, RUNX2, OCN, and ALPL) participating in osteogenic induction at different terms of differentiation was evaluated by real-time PCR. As expected, in untreated samples the expression of COL1A1, RUNX2, OCN, and ALPL was significantly increased starting from day 7 whereas inhibition of their expression was observed in acetoside treated samples. These results suggest that acetoside can regulate the stemness of mesenchymal progenitors by maintaining their undifferentiated state (Figure 7).

Finally, we performed a DCFDA assay to evaluate the antioxidant potential of acetoside in human mesenchymal stem cells (hMSC) with that of (+)-catechin and (-)-epi-catechin, two well-known antioxidant flavonoids. hMSC cells were seeded and pretreated for 4 h with 10 and 100 μ M of catechin, (-)-epi-catechin, and acetoside from *C. phelypaea*. H_2O_2 (1 mM; 3%) was added to the medium for 45', 1.5, and 2 h. As shown in Figure 8, acetoside has a strong antioxidant effect comparable to catechin at the same concentration.

4 | DISCUSSION

Like *Herba Cistanche*, *C. phelypaea* is rich in metabolites with antioxidant activity demonstrating the potential to be used as functional ingredients for foods and nutraceuticals. Our fractionation procedure allowed us to isolate the phenylethanoid glycosides acetoside, 2'-O-acetylacetoside, and tubuloside B, and the iridoid glycosides bartioside, 6-deoxycatalpol, and glucoside. Acetoside and 2'-O-acetylacetoside were the most abundant glycosides we isolated from *C. phelypaea*. The structures of phenylethanoid glycosides were all rich in phenolic hydroxyl groups, which are responsible for the antioxidant activity of *Cistanche* (Zhang et al., 2016).

In human keratinocytes, acetoside had a strong radical scavenging activity that was quite comparable to that of the Trolox, the water-soluble derivative of vitamin E currently used as a control antioxidant standard. Surprisingly, in human mesenchymal progenitor cells, acetoside was still able to efficiently counteract ROS production while Trolox was ineffective.

Skin keratinocytes have a high rate of turnover. The basal proliferative compartment of stratified squamous epithelia consists of the stem and transient amplifying (TA) keratinocytes. Differentiation commitment promotes the withdrawal of keratinocytes from the quiescent stem cell compartment and their transit toward the surface of the tissue. TA keratinocytes transiently acquire appreciable proliferative capacity and

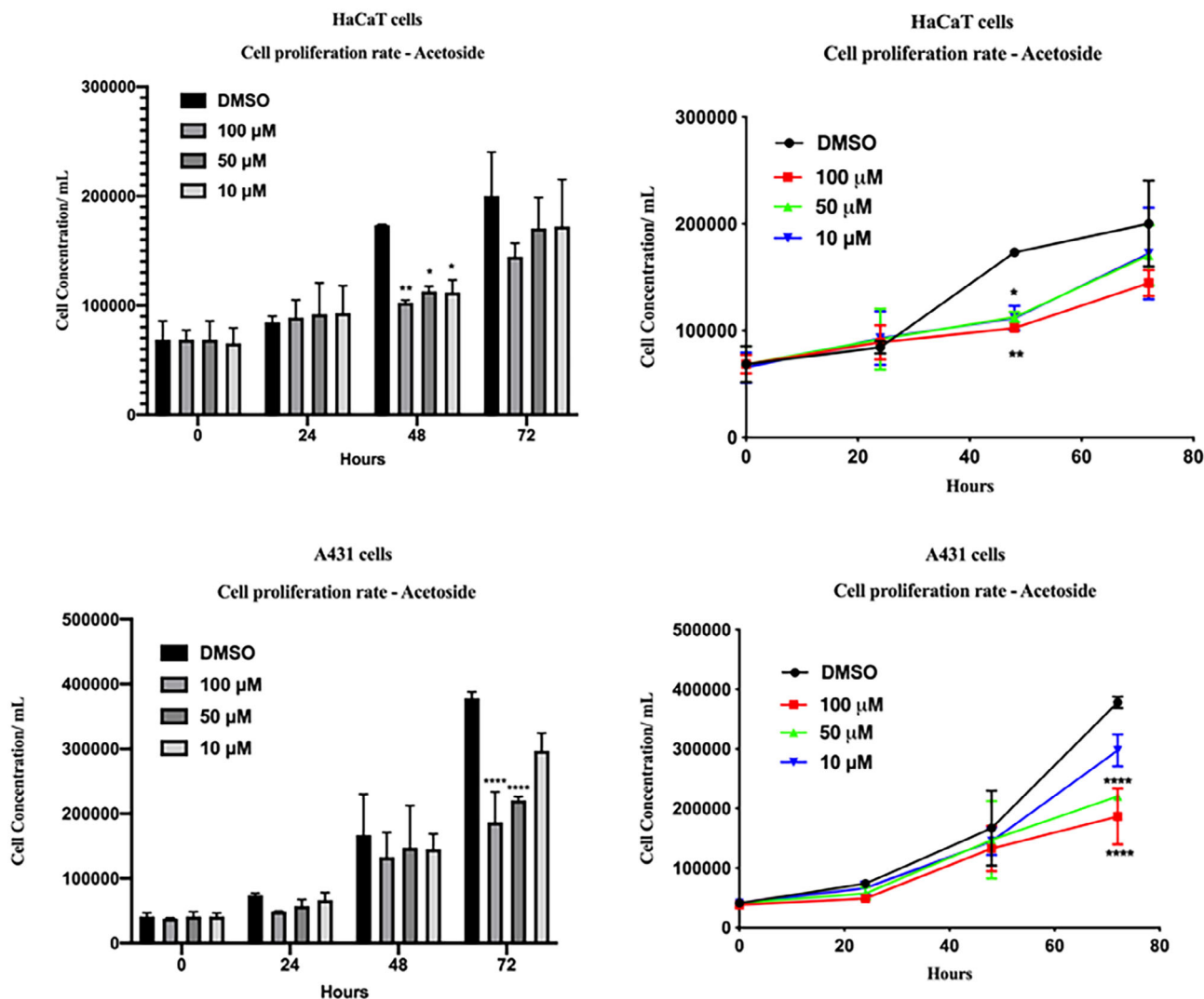


FIGURE 4 Cell proliferation rate. Hacat and A431 cells were seeded and treated with acetoside (1) 10, 50, 100 μ M. Cells were counted with Scepter at T0, 24, 48, 72 h of treatments. Results are the mean \pm SEM of three independent biological experiments relative to the experimental control (DMSO). Statistical analysis was performed with one-way ANOVA, using Dunnett's multiple comparison test. Levels of significance between points of expression are indicated (**** p < 0.001, ** p < 0.01)

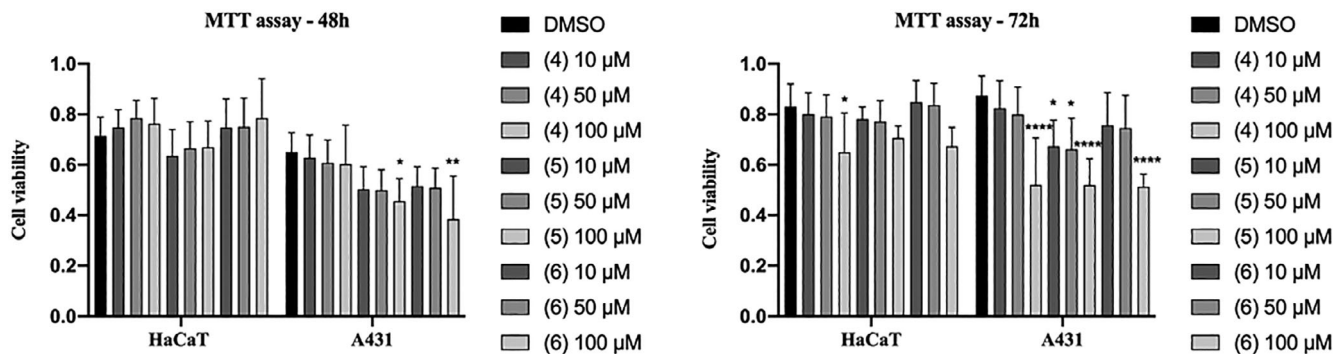


FIGURE 5 MTT viability test. Hacat and A431 cells were incubated with the indicated amounts of metabolites 4, 5, 6, for 24 and 48 h. The values were the mean's six values for each experimental point of two independent biological replicates. Each mean was compared using a Dunnett's multiple comparisons test of ANOVA one-way (p -value * < 0.01, ** < 0.05, *** p < 0.001; **** p < 0.0001)

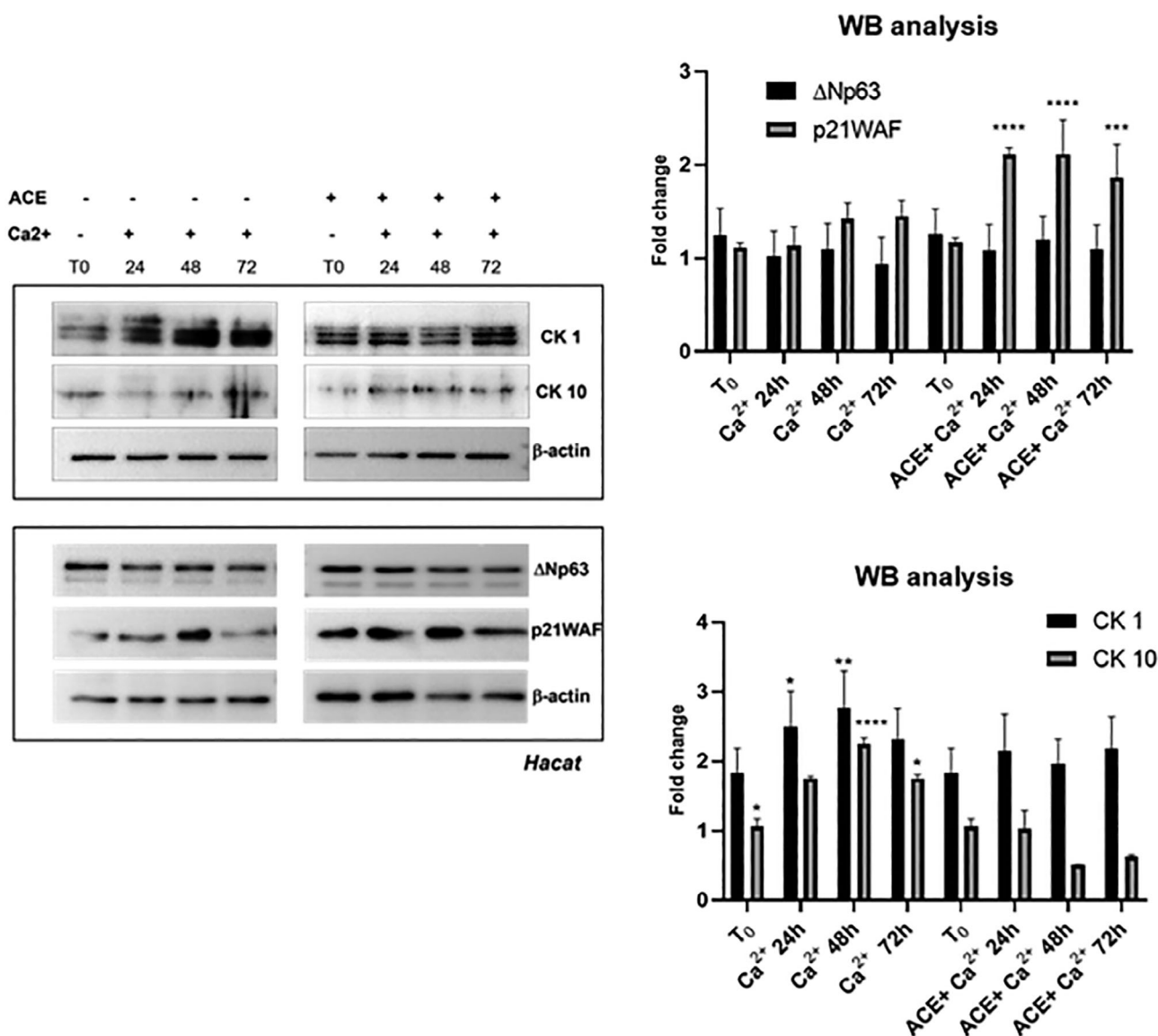


FIGURE 6 Representative western blot analysis of a total extract from Hacat keratinocytes in response to Ca²⁺ addition in the presence or absence of acetoside. Hacat cells were differentiated with 2 mM Ca²⁺ and compared with cells treated with Ca²⁺ plus 50 μM acetoside (ACE) for 48 and 72 h. (a) Immunoblot was probed with ΔNp63α, p21WAF, CK1 and CK10 antibodies. β-Actin was used as a loading control. (b) The signals of protein bands were quantified by ImageLab software version 4.1 (Bio-Rad). Statistical analyses were performed using 2-way ANOVA and Sidak's multiple comparisons or Dunnett's multiple comparisons test. Levels of significance between points of expression are indicated (***p* < 0.001, ***p* < 0.01, **p* < 0.05)

exhibit greatly reduced ΔNp63α. Our data indicate that the co-treatment of human keratinocytes with Ca²⁺, a trigger of keratinocyte differentiation, and acetoside induced a reversible cell cycle arrest. Indeed, in presence of Ca²⁺ and acetoside the expression of p21WAF was upregulated while ΔNp63α, a pro-proliferative marker, was not reduced thus suggesting that acetoside preserves the regenerative potential of keratinocytes. Moreover, in presence of Ca²⁺ and acetoside, cytokeratins 1 and 10 did not increase thereby indicating that keratinocyte differentiation was inhibited or slowed down. On the other hand, it is worth mentioning that acetoside also suppresses macrophages differentiation in osteoclasts without affecting their viability (Lee, Lee, Yi, Kook, & Lee, 2013).

Finally, we found that acetoside inhibited osteoblastic differentiation of hMSCs. hMSCs serve as a primary instrument of tissue engineering. They are multipotent cells with a cell renewal capacity that can differentiate in vitro into a variety of cell types, adipocytes, chondrocytes, and osteoblasts (Okolicsanyi et al., 2015). In addition, they persist in various tissues and are responsible for maintaining tissue homeostasis and repairing tissue injury by replenishing senescent and damaged cells. In general, stem cells are more sensitive than their progeny to the adverse effects of ROS even though a low level of ROS was shown to be required to maintain quiescence and self-renewal of pluripotent stem cells (Zhou, Shao, & Spitz, 2014).

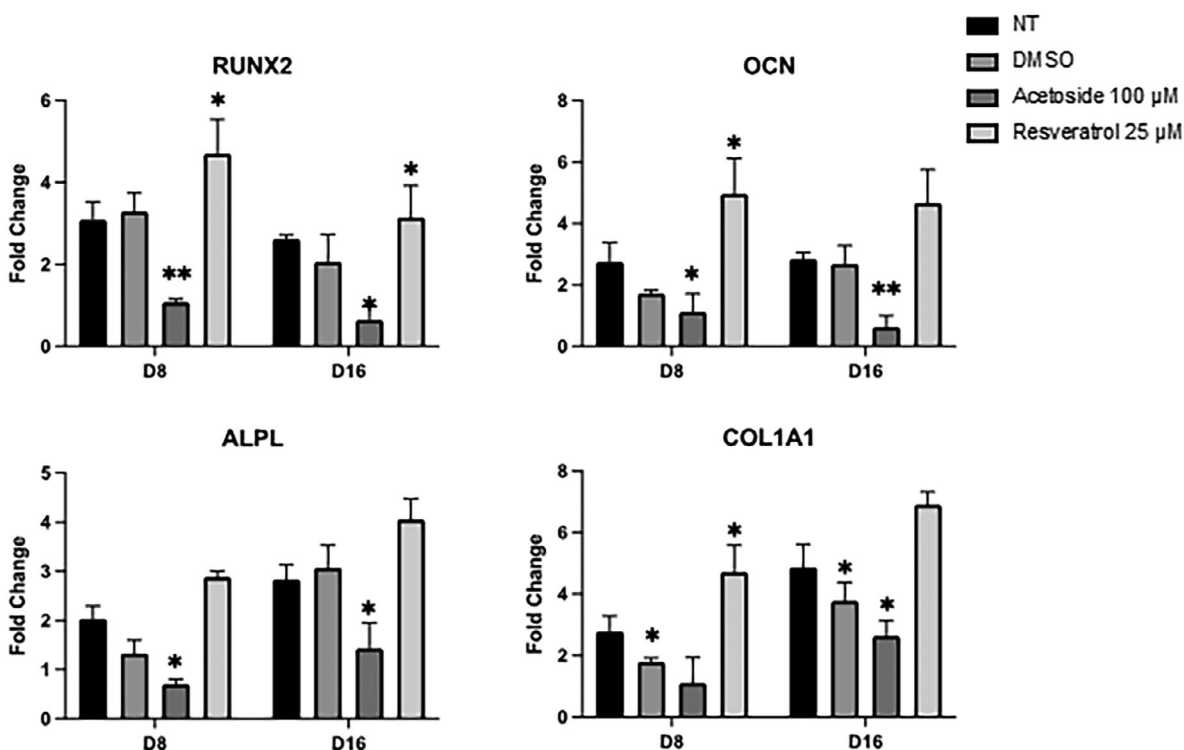


FIGURE 7 RT-qPCR analysis of the osteogenic markers (COL1A1, RUNX2, OCN and ALPL). The mRNA levels were normalized to Gapdh expression and reported as fold change to the value in D0. Resveratrol was used as a positive control of differentiation. The values shown are mean \pm SD, based on triplicate assays. Statistical analyses were performed using Student's *t*-test, where $p < 0.05$ was considered significant ($*p < 0.05$, $**p < 0.01$)

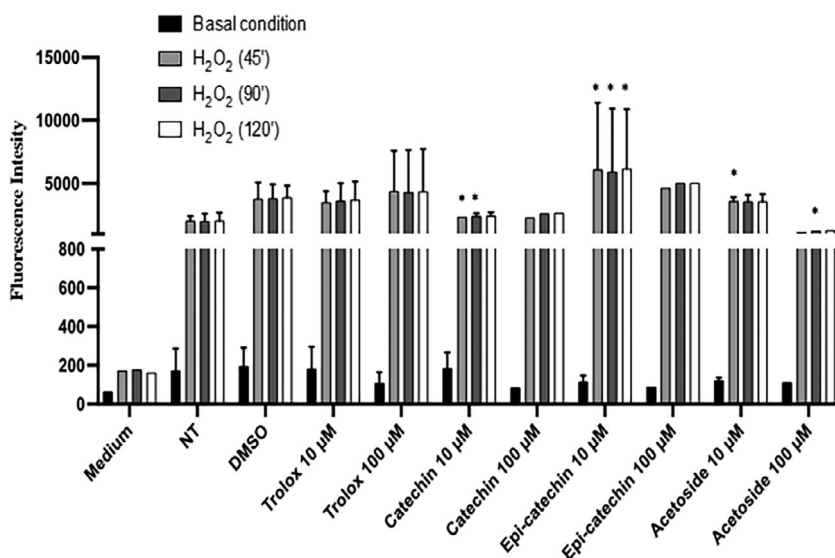


FIGURE 8 DCFDA assay. hMSC cells were seeded and pre-treated for 4 h with 10 and 100 μ M of catechin, *epi*-catechin, and acetoside. H₂O₂ (1 mM; 3%) was added to the medium for 45', 90', and 120'. The fluorescence intensity of DCFDA was read after 45' of incubation. Trolox was used as a positive control and DMSO, in which the metabolites are dissolved, as a negative control. The values are the mean's six values for each experimental point of two independent biological replicates. Statistical analysis was performed with two-way ANOVA, using Tukey's multiple comparison test. Levels of significance between points of expression are indicated ($***p < 0.001$, $**p < 0.01$, $*p < 0.05$)

Excess ROS, instead, can inhibit stem cell self-renewal not only by promoting stem cell differentiation but also via induction of senescence and/or apoptosis. Our data indicate that while controlling ROS production, acetoside preserves the undifferentiated status of mesenchymal stem cells, osteoblasts and osteoclasts precursors. Remarkably, in recent work, total glycosides, and polysaccharides from *C. deserticola* were found to mediate bone formation by

upregulating BMP-2 (Bone Morphogenetic Factor 2) and OPG (Osteoprotegerin) and downregulating RANKL thus promoting the reconstruction of osteoporotic bone (Wang, Tu, Zeng, & Jiang, 2021). Therefore, *Cistanche* extract likely contains metabolites regulating the balance between multipotential mesenchymal stem cells, bone-forming osteoblasts, and bone-resorbing osteoclasts. Therefore, total glycosides and polysaccharides from *Cistanche* are

promising bone-protective therapeutic agents. Further studies will help to clarify the precise activity of each metabolite.

In conclusion, besides its strong antioxidant potential, acetoside appears to preserve the proliferative potential of human basal keratinocyte and mesenchymal progenitors which is necessary for tissue morphogenesis and renewal. The use of stem cells in tissue engineering demands their controlled differentiation; hMSCs have great therapeutic potential, however, their usefulness is limited by cellular senescence occurring secondary to increased levels of reactive oxygen species during their propagation in culture (Ogrodnik et al., 2017). To this respect, acetoside can be of practical relevance for the clinical application of human stem cell cultures for regenerative medicine.

ACKNOWLEDGMENTS

A. Evidente is associated to the Istituto di Chimica Biomolecolare del CNR, Italy. Open Access Funding provided by Università degli Studi di Napoli Federico II within the CRUI-CARE Agreement.

CONFLICT OF INTEREST

The authors declare no conflict of interest.

DATA AVAILABILITY STATEMENT

The data supporting this study's findings are available from the corresponding author upon reasonable request.

ORCID

Antonella Delicato  <https://orcid.org/0000-0002-8268-2038>

Viola Calabrò  <https://orcid.org/0000-0002-6508-8889>

REFERENCES

- Aligiannis, N., Mitaku, S., Tsitsa-Tsardis, E., Harvala, C., Tsaknis, I., Lalas, S., & Haroutounian, S. (2003). Methanolic extract of *Verbascum macrurum* as a source of natural preservatives against oxidative rancidity. *Journal of Agricultural and Food Chemistry*, 51, 7308–7312.
- Amoresano, A., Di Costanzo, A., Leo, G., Di Cunto, F., La Mantia, G., Guerrini, L., & Calabro, V. (2010). Identification of Δ Np63 α protein interactions by mass spectrometry. *Journal of Proteome Research*, 9, 2042–2048.
- Arslanian, R. L., Harris, G. H., & Stermitz, F. R. (1985). Some iridoid glycosides, including the new 6-deoxycatalpol, from Indian paintbrush species related to *Castilleja miniata*. *Journal of Natural Products*, 48, 957–961.
- Bougandoura, A., D'Abrosca, B., Ameddah, S., Scognamiglio, M., Mekkiou, R., Fiorentino, A., ... Benayache, F. (2016). Chemical constituents and in vitro anti-inflammatory activity of *Cistanche violacea* Desf. (Orobanchaceae) extract. *Filoterapia*, 109, 248–253.
- Cimmino, A., Mathieu, V., Evidente, M., Ferderin, M., Banuls, L. M. Y., Masi, M., ... Evidente, A. (2016). Glanduliferins A and B, two new glucosylated steroids from *Impatiens glandulifera*, with in vitro growth inhibitory activity in human cancer cells. *Filoterapia*, 109, 138–145.
- Dewick, P. M. (2009). *Medicinal natural products* (3rd ed.). Chichester, UK: John Wiley and Sons Ltd.
- Deyama, T., Yahikozawa, K., Al-Easa, H. S., & Rizk, A. M. (1995). Constituents of plants growing in Qatar: Part xxviii. *Constituents of Cistanche Phelypaea*. <http://hdl.handle.net/10576/9781>
- di Martino, O., Troiano, A., Guarino, A. M., Pollice, A., Vivo, M., La Mantia, G., & Calabrò, V. (2016). Δ Np63 α controls YB-1 protein stability: Evidence on YB-1 as a new player in keratinocyte differentiation. *Genes to Cells*, 21, 648–660.
- Gast, M. (2000). *Moissons du désert. Utilisation des ressources naturelles au Sahara central*. Paris: Ibis Press 160 p. voir la notice.
- Gu, C., Yang, X., & Huang, L. (2016). Cistanches Herba: A neuropharmacology review. *Frontiers in Pharmacology*, 7, 289.
- Han, L., Ji, L., Boakye-Yiadom, M., Li, W., Song, X., & Gao, X. (2012). Preparative isolation and purification of four compounds from *Cistanches deserticola* YC Ma by high-speed counter-current chromatography. *Molecules*, 17, 8276–8284.
- Kim, K. H., Kim, S., Jung, M. Y., Ham, I. H., & Whang, W. K. (2009). Anti-inflammatory phenylpropanoid glycosides from *Clerodendron trichotomum* leaves. *Archives of Pharmacological Research*, 32, 7–13.
- Kobayashi, H., Karasawa, H., Miyase, T., & Fukushima, S. (1985). Studies on the constituents of Cistanche herba. VI. Isolation and structure of a new iridoid glycoside, 6-deoxycatalpol. *Chemical and Pharmaceutical Bulletin*, 33, 3645–3650.
- Kobayashi, H., Oguchi, H., Takizawa, N., Miyase, T., Ueno, A., Usmanghani, K., & Ahmad, M. (1987). New Phenylethanoid glycosides from *Cistanche tubulosa* (SCHRENK) HOOK. F.I. *Chemical and Pharmaceutical Bulletin*, 35, 3309–3314.
- Lakhdari, W., Dehliz, A., Acheuk, F., Mlik, R., Hammi, H., Doumandji-Mitiche, B., & Chergui, S. (2016). Ethnobotanical study of some plants used in traditional medicine in the region of Oued Righ (Algerian Sahara). *Journal of Medicinal Plant Studies*, 4, 204–211.
- Lee, S. Y., Lee, K. S., Yi, S. H., Kook, S. H., & Lee, J. C. (2013). Acteoside suppresses RANKL-mediated osteoclastogenesis by inhibiting c-Fos induction and NF- κ B pathway and attenuating ROS production. *PLoS One*, 8, e80873.
- Li, Y., Ishibashi, M., Satake, M., Oshima, Y., & Ohizumi, Y. (2003). A new iridoid glycoside with nerve growth factor-potentiating activity, gelsemiol 6'-trans-caffeoyl-1-glucoside, from *Verbena littoralis*. *Chemical and Pharmaceutical Bulletin*, 51, 1103–1105.
- Li, H., Jiang, H., & Liu, J. (2017). Traditional Chinese medical therapy for erectile dysfunction. *Translational Andrology and Urology*, 6, 192–198.
- Li, X., Xie, Y., Li, K., Wu, A., Xie, H., Guo, Q., ... Chen, D. (2018). Antioxidation and Cytoprotection of Acteoside and its derivatives: Comparison and mechanistic chemistry. *Molecules*, 23, 498.
- López-Espinosa, J.A. 2022. *Cistanche Phelypaea*. https://www.regmurcia.com/servlet/s.SI?sit=a,0,c,365,m,1309&r=ReP-29346-DETALLE_REPORTAJES. Accessed March 22, 2022.
- Melek, F. R., El-Shabrawy, O. A., El-Gindy, M., & Miyase, T. (1993). Pharmacological activity and composition of ethyl acetate extract of *Cistanche phelypaea*. *Fitoterapia*, 64, 11.
- Morikawa, T., Xie, H., Pan, Y., Ninomiya, K., Yuan, D., Jia, X., ... Muraoka, O. (2019). A review of biologically active natural products from a desert plant *Cistanche tubulosa*. *Chemical and Pharmaceutical Bulletin*, 67, 675–689.
- Ogrodnik, M., Miwa, S., Tchkonja, T., Tiniakos, D., Wilson, C. L., Lahat, A., & Jurk, D. (2017). Cellular senescence drives age-dependent hepatic steatosis. *Nature Communications*, 8, 1–12.
- Okolicsanyi, R. K., Camilleri, E. T., Oikari, L. E., Yu, C., Cool, S. M., Van Wijnen, A. J., & Haupt, L. M. (2015). Human mesenchymal stem cells retain multilineage differentiation capacity including neural marker expression after extended in vitro expansion. *PLoS One*, 10, e0137255.
- Pujadas-Salvá, A.J., & López-Saéz, J.A. (2002). Cistanche. In: López-Sáez, J. A., Catalán, P. & Sáez, L. (Eds.), *Plantas parásitas de la Península Ibérica e Islas Baleares* (pp. 440–451). Madrid, Spain: Editorial Mundi-Prensa.
- Qiao, Z., Tang, J., Wu, W., Tang, J., & Liu, M. (2019). Acteoside inhibits inflammatory response via JAK/STAT signaling pathway in osteoarthritis rats. *BMC Complementary and Alternative Medicine*, 19, 264.
- Salehi, M., Esmailzadeh, S. H., Kheyli, S. A. G., Malekshah, A. F., & Zaroudi, M. (2019). *Cistanche tubulosa* could be considered as medicinal plant in halophytes farming. In R. Tucker (Ed.), *Halophytes* (pp. 193–233). New York, NY: Nova Science Publishers, Inc.

- Song, Y., Zeng, K., Jiang, Y., & Tu, P. (2021). *Cistanches Herba*, from an endangered species to a big brand of Chinese medicine. *Medicinal Research Reviews*, 41, 1539–1577.
- Sticher, O., & Weisflog, A. (1975). Detection and isolation of the iridoid glucoside of *Galeopsis tetrahit* L. (Labiatae) as well as elucidation of the structure of glucoside. *Pharmaceutica Acta Helveticae*, 50, 394–403.
- Thorogood, C. J., Leon, C. J., Lei, D., Adughayman, M., Huan, L.-F., & Hawkins, J. A. (2021). Desert hyacinths: An obscure solution to a global problem. *Plants, People, Planet*, 3, 302–307.
- Tian, X. Y., Li, M. X., Lin, T., Qiu, Y., Zhu, Y. T., Li, X. L., & Chen, L. P. (2021). A review on the structure and pharmacological activity of phenylethanoid glycosides. *European Journal of Medicinal Chemistry*, 209, 112563.
- Trampetti, F., Pereira, C., Rodrigues, M. J., Celaj, O., D'Abrosca, B., Zengin, G., ... Custódio, L. (2019). Exploring the halophyte *Cistanche phelypaea* (L.) Cout as a source of health-promoting products: In vitro antioxidant and enzyme inhibitory properties, metabolomic profile and computational studies. *Journal of Pharmaceutical and Biomedical Analysis*, 165, 119–128.
- Van Meerloo, J., Kaspers, G. J. L., & Cloos, J. (2011). Cell sensitivity assays: The MTT assay. *Methods in Molecular Biology*, 731, 237–245.
- Venditti, A., Serrilli, A. M., & Bianco, A. (2013). Iridoids from *Bellardia trixago* (L.) all. *Natural Product Research*, 27, 1413–1416.
- Vivo, M., Fontana, R., Ranieri, M., Capasso, G., Angrisano, T., Pollice, A., ... La Mantia, G. (2017). p14ARF interacts with the focal adhesion kinase and protects cells from anoikis. *Oncogene*, 36, 4913–4928.
- Volpato, G., Saleh, S. M. L., & Di Nardo, A. (2015). Ethnoveterinary of Sahrawi pastoralists of Western Sahara: Camel diseases and remedies. *Journal of Ethnobiology and Ethnomedicine*, 11, 54.
- Wang, C., Gong, X., Bo, A., Zhang, L., Zhang, M., Zang, E., & Li, M. (2020). Iridoids: Research advances in their phytochemistry, biological activities, and pharmacokinetics. *Molecules*, 25, 287.
- Wang, F., Tu, P., Zeng, K., & Jiang, Y. (2021). Total glycosides and polysaccharides of *Cistanche deserticola* prevent osteoporosis by activating Wnt/ β -catenin signaling pathway in SAMP6 mice. *Journal of Ethnopharmacology*, 271, 113899.
- Wang, Y. E., Zhang, L. I., Du, Z., Pei, J., & Huang, L. (2019). Chemical diversity and prediction of potential cultivation areas of *Cistanche* herbs. *Scientific Reports*, 9, 19737.
- Wang, Y. J., Zhou, S. M., Xu, G., & Gao, Y. Q. (2015). Interference of phenylethanoid glycosides from *Cistanche tubulosa* with the MTT assay. *Molecules*, 20, 8060–8071.
- Warren, S. (2015). Trypan blue exclusion test of cell viability. *Current Protocol Immunology*, 111, A3.B.1–A3.B.3.
- Xiao, D., Powolny, A. A., & Singh, S. V. (2008). Benzyl isothiocyanate targets mitochondrial respiratory chain to trigger reactive oxygen species-dependent apoptosis in human breast cancer cells. *Journal of Biological Chemistry*, 283, 30151–30163.
- Xu, R., Chen, J., Chen, S. L., Liu, T. N., Zhu, W. C., & Xu, J. (2009). *Cistanche deserticola* Ma cultivated as a new crop in China. *Genetic Resources and Crop Evolution*, 56, 137–142.
- Yang, L., Zhang, B., Liu, J., Dong, Y., Li, Y., Li, N., ... Ma, X. (2019). Protective effect of Acteoside on Ovariectomy-induced bone loss in mice. *International Journal of Molecular Sciences*, 20(12), 2974.
- Yoshizawa, F., Deyama, T., Takizawa, N., Usmanghani, K., & Ahmad, M. (1990). The constituents of *Cistanche tubulosa* (SCHRENK) HOOK. f. II: Isolation and structures of a new phenylethanoid glycoside and a new neolignan glycoside. *Chemical and Pharmaceutical Bulletin*, 38, 1927–1930.
- Zhang, W., Huang, J., Wang, W., Li, Q., Chen, Y., Feng, W., Zheng, D., Zhao, T., Mao, G., Yang, L., Wu, X. (2016) Extraction, purification, characterization and antioxidant activities of polysaccharides from *Cistanche tubulosa*. *International Journal of Biological Macromolecules*, 93, 448–458.
- Zhang, C. Z., Wang, S. X., Zhang, Y., Chen, J. P., & Liang, X. M. (2005). In vitro estrogenic activities of Chinese medicinal plants traditionally used for the management of menopausal symptoms. *Journal of Ethnopharmacology*, 98, 295–300.
- Zhou, D., Shao, L., & Spitz, D. R. (2014). Chapter one – Reactive oxygen species in normal and tumor stem cells. *Advances in Cancer Research*, 122, 1–67.

How to cite this article: Delicato, A., Masi, M., de Lara, F., Rubiales, D., Paolillo, I., Lucci, V., Falco, G., Calabrò, V., & Evidente, A. (2022). In vitro characterization of iridoid and phenylethanoid glycosides from *Cistanche phelypaea* for nutraceutical and pharmacological applications. *Phytotherapy Research*, 1–12. <https://doi.org/10.1002/ptr.7548>